

Activation of Hedgehog pathway by circEEF2/miR-625-5p/TRPM2 axis promotes prostate cancer cell proliferation through mitochondrial stress

ChenHui Zhu,¹ LiJuan Lin,² ChangQing Huang,¹ ZhiHui Wu¹

¹Department of Urology;

²Department of Anaesthesia, Central People's Hospital of Zhanjiang, Zhanjiang City, Guangdong Province, China

ABSTRACT

The purpose of this study was to identify the role played by circEEF2 (has-circ-0048559) in prostate cancer (PCa) development and to determine the potential mechanism involved. circEEF2, miR-625-5p, and the transient receptor potential M2 channel protein (TRPM2) were determined using RT-qPCR in PCa. Cell proliferation was determined by CCK-8 assay and colony formation assay, whereas migration and invasion were assessed by transwell assay, and apoptosis was evaluated by flow cytometry after annexin V-FITC and propidium iodide staining. The interactions between circEEF2 and miRNAs were investigated through the Circular RNA Interactome database, and the downstream targets of miR-625-5p were forecasted using TargetScan. The interaction was confirmed using both the dual luciferase reporter gene assay and RNA pull-down assay. TRPM2, Hedgehog signaling pathway proteins (GLI1 and GLI2), ubiquinone oxidase subunit B8, and cytochrome C oxidase subunit IV (COX4) were analyzed by protein blotting. JC-1 fluorescence detection was applied for mitochondrial membrane potential changes, fluorescent probe assay for intracellular ROS levels, and immunofluorescence staining for γ -H2AX expression. The role of circEEF2 in PCa tumor growth was tested by xenograft experiments. CircEEF2 expression was upregulated in PCa ($p < 0.05$). Cells of PCa were inhibited in proliferation, migration, invasion, and enhanced in apoptosis by depleting circEEF2 ($p < 0.05$). circEEF2 directly targeted adsorbed miR-625-5p. TRPM2 bound to miR-625-5p. Upregulating TRPM2 likewise reversed the therapeutic effect of depleting circEEF2 on cancer development in PCa cells. circEEF2 activates the Hedgehog pathway through the miR-625-5p/TRPM2 axis, promotes mitochondrial stress, and promotes PCa development *in vivo*. circEEF2 upregulates mitochondrial stress to promote PCa by activating the Hedgehog pathway through the miR-625-5p/TRPM2 axis.

Key words: circEEF2; miR-625-5p; TRPM2; Hedgehog signaling pathway; mitochondrial stress; prostate cancer.

Correspondence: ZhiHui Wu, Department of Urology, Central People's Hospital of Zhanjiang, No.236, Yuanzhu Road, Chikan District, Zhanjiang City 524037, Guangdong Province, China. E-mail: wuzhihui1989@outlook.com

Contributions: CHZ, research study design, manuscript original drafting; CHZ, LJJ, research performing, data analysis; CQH, ZHW, research assistance and advice; ZHW, manuscript review and editing. All authors contributed to editorial changes in the manuscript, read and approved the final manuscript and agreed to be accountable for all aspects of the work.

Conflict of interest: the authors declare no conflicts of interest related to this work.

Ethics approval: the present study was approved by the Ethics Committee of Central People's Hospital of Zhanjiang (No.202003ZJ93) and written informed consent was provided by all patients prior to the study start. All procedures were performed in accordance with the ethical standards of the Institutional Review Board and The Declaration of Helsinki, and its later amendments or comparable ethical standards. All animal experiments were complied with the ARRIVE guidelines and performed in accordance with the National Institutes of Health Guide for the Care and Use of Laboratory Animals. The experiments were approved by the Institutional Animal Care and Use Committee of Central People's Hospital of Zhanjiang (No.202005Z660).

Availability of data and materials: the data used to support the findings of this study are available from the corresponding author upon request.

Introduction

Prostate cancer (PCa) is the most prevalent malignancy among men,¹ accounting for 27% of cancer cases with a mortality rate second only to lung cancer.² Currently, standard treatments for PCa include surgery, radiotherapy, endocrine therapy, and chemotherapy; however, these conventional treatment options have limited success.³ Due to uncontrolled proliferation and metastasis of PCa cells, the median survival of PCa patients is only 2-3 years with conventional prostatectomy and androgen deprivation therapy.^{4,5} Therefore, novel biomarkers for PCa therapy and their underlying molecular mechanisms are urgently needed. Circular RNAs (circRNAs) are non-coding RNAs containing specific ring structures with covalent bonds,⁶ which are evolutionarily conserved, stable, abundant, and tissue-specific, and their regulatory roles are involved in cancer genesis and progression.⁷ circRNAs are differentially expressed in a wide range of malignant tumors and have been associated with tumorigenesis.⁸⁻¹¹ In PCa, circRNA_100395 prevents cell proliferation, alters cell cycle distribution, and decreases cell migration and invasive ability.⁴ circ_0006404 accelerates PCa cell survival and proliferation, while hindering PCa cell apoptosis.¹² circFOXO3 impedes cell viability and metastasis in PCa cells.¹³ Some circRNAs can play biological roles in PCa development as microRNAs (miRNAs) competing endogenous RNA (ceRNA).¹⁴ circRNAs are capable of focusing on the absorption of miRNAs, thereby influencing the binding to specific genes and indirectly enhancing the expression of those genes.¹⁵ circEEF2 is an upregulated target in ovarian cancer and promotes autophagy through the interaction of miR-6881-3p and ANXA2.¹⁶

miRNAs are considered to play a major role as tumor suppressor genes, and their dysregulation is currently considered to be a common feature of human cancer, and their reduction or inhibition will lead to tumor formation.^{17,18} miRNAs play a key role in regulating gene expression by binding to mRNA, thereby affecting protein production and downstream cell function.¹⁹ As a member of the miRNA family, miR-625-5p plays an important role in a variety of cancers including PCa.²⁰⁻²³

Transient receptor potential melastatin 2 (TRPM2) is a calcium permeable ion channel, which is considered to be a prognostic marker of PCa and an important regulator of autophagy.²⁴ However, the regulation of circEEF2 on miR-625-5p/TRPM2 in PCa is not clear. The Hedgehog (Hh) pathway plays a pivotal role in embryonic development stages, encompassing cell growth, differentiation, and organogenesis.²⁵ In fact, Hh signaling is vital in the progression of PCa to more severe or drug-resistant conditions.²⁶ Abnormal mitochondrial function has also been found to be associated with disease progression and metastasis in PCa studies.²⁷ Mitochondria play a key role in PCa, including abnormalities in metabolic function, mitochondrial fission, and mitochondrial DNA mutations.²⁸ These findings provide new ideas and possible targets for PCa treatment.

This study focuses on how circEEF2 activates the Hh signaling pathway through the miR-625-5p/TRPM2 axis, and how it promotes the proliferation of PCa cells through mitochondrial stress mechanisms, with the aim to provide new targets and strategies for the treatment of PCa.

Materials and Methods

Clinical samples

This study was conducted with the approval of the Ethics Committee of Central People's Hospital of Zhanjiang (authoriza-

tion no. 202003ZJ93). A total of 30 pairs of PCa tissues and paracancerous tissues were surgically removed from 30 patients with PCa who received prostatectomy. No subject had received chemotherapy or radiotherapy prior to radical resection. PCa and paracancerous tissue specimens were stored at -80°C.

Cell culture

The human normal prostate epithelial cell line RWPE-1 and PCa cell lines (22Rv1, PC3, Du145) were obtained from the National Collection of Authenticated Cell Cultures (Shanghai, China). The cultivation of RWPE-1 was conducted using K-SFM medium (Gibco, Waltham, MA, USA), Dulbecco's modified Eagle's medium (Gibco) for PC3 and Du145 cells, whereas RPMI-1640 (Gibco) for 22Rv1 cells. With the medium filled with 10% fetal bovine serum, 100 U/mL penicillin, and 100 mg/mL streptomycin, cells were kept under 5% CO₂.

Cell transfection

GenePharma (Shanghai, China) synthesized small interfering RNA targeting circEEF2 (si-circEEF2, sequence: GCCGAGATG-TATGTGAACTTC) and negative control siRNA (si-NC), along with TRPM2 overexpression plasmid (pcDNA3.1-TRPM2) and empty plasmid (pcDNA3.1-NC), miR-625-5p mimic, miR-625-5p inhibitor, mimic NC, and inhibitor NC. Upon attaining 80% confluence, PC3 cells were transfected with plasmids or oligonucleotides using Lipofectamine™ 3000 (Invitrogen, Waltham, MA, USA). RT-qPCR was employed to ascertain the efficiency of the transfection.

Nucleoplasmic separation assay and RNase R assay

RNA specimens from both cytoplasmic and nuclear segments of PC3 cells were extracted utilizing the PARIS™ Kit Protein and RNA Isolation System Kit (Thermo Fisher Scientific, Waltham, MA, USA). circEEF2 within the nucleus and cytoplasm was ascertained through RT-qPCR analysis. RNA (5 µg), isolated from cells with TRIzol reagent, underwent a 30-min incubation at 37°C with 20 U/µL RNase R (3 U/µg RNA; LGC Biosearch Technologies, Middleton, WI, USA). Controls were treated without RNase R. circEEF2 and linear EEF2 were determined using RT-qPCR.

CCK-8 assay

CCK-8 assay (Raffles Bio, Nanjing, China) was used for the measurement of PC3 cell proliferation. Briefly, 48 h after transfection, a total of 3×10^3 cells were inoculated using a 48-well plate and incubated at 37°C. At 0, 24, 48, and 72 h, each well received an addition of 15 µL of CCK-8 (8 mg/mL). Absorbance at 450 nm was measured following an hour of incubation at 37°C, utilizing a microplate reader.

JC-1 detection

The BD MitoScreen Kit (BD Pharmingen, San Diego, CA, USA) was utilized to conduct the JC-1 test. Briefly, after transfection, PC3 cells were cultured in Petri dishes at 2×10^5 cells/well. After 24 h, cells were harvested and kept with JC-1 reagent (100 ng/mL) for 15 min. Flow cytometry (BD Biosciences) analysis was then performed.

ROS detection

The cells underwent transfection for 48 h, followed by a 20-min incubation at 37°C in a medium with 10 µM DCFH-DA. Post-PBS wash, cell fluorescence was quickly observed using an inverted fluorescence microscope, distinguished by its excitation wavelength of 485 nm and emission wavelength of 530 nm. Green fluorescence intensity was gauged using the image analysis tool, Cell Quest Program.

Immunofluorescence staining

PC3 cells underwent fixation using 4% paraformaldehyde for 20 min, were permeated with 0.4% Triton X-100 for 1 h, and then treated with goat serum for 1 h. Subsequently, they were stained overnight at 4°C with the primary antibody targeting γ -H2AX (ab195189, 1:200, Abcam, Waltham, MA, USA). Post a PBS rinse, PC3 cells underwent a 1-h incubation with Alexa Fluor 647 linked secondary antibody (ab150079, 1:200, Abcam), followed by a 5-min DAPI staining (Beyotime Biotech, Haimen, China). As a negative control, only the antibody diluent was used instead of the primary antibody. Confocal microscopy (FV1000; Olympus Corporation, Tokyo, Japan) was conducted to observe cells. Image J software was used to quantify the region of each γ -H2AX focus.

Transwell assays

Migration assay: 24 h post-transfection, the upper compartment received PC3 cells (1×10^4 cells/well) in a serum-free environment, whereas the lower compartment was filled with a medium enriched with 10% FBS. Following a 24-h period, PC3 cells that had migrated were stained using crystal violet (Sigma-Aldrich, St. Louis, MO, USA) and tallied.

Invasion assay: the upper compartment was covered with Matrigel® (Millipore, Burlington, MA, USA), in which the transfected PC3 cells (5×10^4 cells/well) were inoculated. In the same way as in the cell migration assay, the rest of the steps were repeated. Five random light fields were imaged using a microscope (Nikon, Tokyo, Japan) and the number of migrated cells was counted.

Flow cytometric assessment of apoptotic cells

The Annexin V-FITC Apoptosis Kit (Solarbio, Beijing, China) was utilized to perform the apoptosis assay. After transfection, PC3 cells (10^5 cells/well) were added to 12-well plates and incubated for 48 h. The cells underwent trypsin digestion, were reconstituted in a binding buffer, and then treated with 10 μ L of Annexin V-FITC and propidium iodide for 10 min. The measurement of stained cells was conducted using flow cytometry (Agilent, Hangzhou, China).

Colony formation assay

Following a 24-h transfection period, PC3 cells were introduced into 6 cm dishes, maintaining a density of 300 cells per well, and then incubated for a fortnight at 37°C with 5% CO₂. Following a fortnight, the supernatant was discarded, and the cells underwent a 20-min staining process using crystal violet. The number of colony formations was counted under a microscope (Nikon, Tokyo, Japan).

FISH assay

According to the FISH kit instructions (GenePharma, Shanghai, China), hybridization of circEEF2 was performed using a Cy2-labeled probe and miR-625-5p using a Cy5-labeled probe (GenePharma). Then 100 μ L of diluted DAPI was added and the

cells were stained in the dark for 15 min, washed with PBS, and sealed. Confocal laser scanning microscope (FV1000; Olympus) was utilized to observe the subcellular distribution of circEEF2 and miR-625-5p in PC3 cells.

Dual luciferase reporter gene assay

Potential binding sites between miR-625-5p with circEEF2, TRPM2 3'UTR were predicted at starbase (<https://rnasysu.com/encori/>) and TargetScan (<https://www.targetscan.org/>). Partial fragments of the 3'UTR of circEEF2 or TRPM2, including sequences that bind to the wild type or mutant of miR-625-5p, were cloned into the pmirGLO luciferase vector (GenePharma). The miR-625-5p mimic or miR-NC was cotransfected with the luciferase reporter into PC3 cells using Lipofectamine™ 3000 for 48 h. Then, luciferase activity was analyzed using the Luciferase Reporter Gene Assay System kit (Promega, Madison, WI, USA).

RNA pull down

Biotin-labeled miR-625-5p and the corresponding NC probe (GenePharma) were incubated with streptavidin-coated beads for 3 h. For 12 h at 4°C, biotin-miR-625-5p probe was incubated with lysed PC3 cells. After elution from the beads, the complexes were purified with TRIzol, and circEEF2 and TRPM2 were assessed using RT-qPCR.

RT-qPCR

Using TRIzol reagent (Thermo Fisher Scientific), total RNA was isolated from either tumor tissues or PC3 cells. The RT-qPCR process utilized the PrimeScript™ RT Kit (Takara Bio Inc., Kusatsu, Japan) alongside the Mir-XTM miRNA RT-qPCR SYBR® Kit (Takara). A quantity equal to 1 μ g of total RNA was converted into cDNA. The presence of mRNA and miRNA in specific genes was identified through RT-qPCR on an ABI-7900 system, utilizing SYBR Green (Takara). Target genes were normalized to GAPDH or U6. The primer sequences are presented in Table 1.

Western blotting

Proteins were extracted from cells and tumor tissues using RIPA buffer supplemented with protease inhibitors (Beyotime). The BCA method (Pierce; Thermo Fisher Scientific) was taken to detect the amount of protein. Proteins (20 μ g) were separated by SDS-PAGE and then transferred to a nitrocellulose membrane (Millipore). After sealing in 5% skimmed milk powder, the membranes were incubated at 4°C with the following primary antibodies: TRPM2 (1:300, ab11168, Abcam), GLI1 (1:1000, ab134906, Abcam), GLI2 (1:500, ab187386, Abcam), NDUFB8 (1:1000, ab110242, Abcam), COX4 (1:1000, ab110272, Abcam), E-Cadherin (1:500, ab40772, Abcam), vimentin (1:1000, ab92547, Abcam) and GAPDH (1:1000, #5174, Cell Signaling Technology, USA) overnight. Specific proteins were combined with

Table 1. Sequences of primers.

circEEF2	GATCGATCCTGTCCTCGGTA	GACAGACATGTTGCGGATGT
linear EEF2	TCAAACCTGGACAGCGAGGAC	TCTACTTCTCGGCCAGGTA
miR-625-5p	AGGGGAAAGTTCTATAGTCC	GCAGGGTCCGAGGTATTC
TRPM2	CCGAGCAGAAGATCGAGGAC	GGGTGGTTACTGGAGCCTTC
GAPDH	CACCCACTCCTCCACCTTTG	CCACCACCCTGTTGCTGTAG
U6	CTCGCTTCGGCAGCAC	AACGCTTCACGAATTTGCGT

circEEF2, circular RNA eukaryotic elongation factor 2; TRPM2, transient receptor potential (melastatin) 2; GAPDH, Glyceraldehyde-3-phosphate dehydrogenase.

horseradish peroxidase-labeled secondary antibody (1:1000, #ab124055, Abcam), which was incubated for 2 h. Protein signals were developed using the ECL kit (Thermo Fisher Science) in a chemiluminescence imager (Image Quant LAS4000 mini, GE Healthcare, Hatfield, UK) and analyzed using Image J software.

In vivo xenotransplantation

Nude BALB/c mice, aged 5 weeks and male, were acquired from the Beijing Experimental Animal Research Center in Beijing, China. RiboBio (Guangzhou, China) created lentiviral vectors for short hairpin RNA targeting circEEF2 (sh-circEEF2) or NC (sh-NC). PC3 cells underwent transfection using sh-circEEF2 or sh-NC, followed by the selection of cells with stable transfection using puromycin. A total of 5×10^6 PC3 cells, consistently transfected with either sh-circEEF2 or sh-NC, were administered subcutaneously into the sides of mice, with six in each group. Over a period of 4 weeks, tumor sizes were assessed on a weekly basis, with the calculation being volume (mm^3) = length \times width²/2. Under the influence of isoflurane anesthesia, mice underwent euthanasia through cervical dislocation. After weighing the tumor samples, they were utilized to measure TRPM2, GLI1, and GLI2. Animal experiments were approved by the Central People's Hospital of Zhanjiang Animal Management and Use Committee (authorization no.202005Z660).

Data statistics

An analysis of the data was carried out using GraphPad Prism 8.0 (GraphPad, La Jolla, CA, USA). Experiments were conducted on three separate occasions. Data are expressed as mean \pm SD. Differences were compared using Student's *t*-test or ANOVA with Tukey's *post-hoc* test. Statistics were considered significant at $p < 0.05$.

Results

circEEF2 is highly expressed in PCa

To detect circEEF2 in PCa, the abundance of circEEF2 was detected in 30 pairs of PCa tumor tissues and paracancerous tissues using RT-qPCR. circEEF2 level was upregulated in PCa tumor tissues compared with paracancerous tissues (Figure 1A) and in PCa cell lines (22Rv1, PC3, Du145) compared to RWPE-1 (Figure 1B). Given the highest expression of circEEF2 in PC3, subsequent studies were performed in PC3 cells. Furthermore, nucleoplasmic separation assays showed that PC3 cells predominantly contained circEEF2 in the cytoplasm (Figure 1C). The stability of circEEF2 in PC3 cells was examined by RNase R digestion. RNase R treatment significantly decreased the mRNA level of linear EEF2, while circEEF2 expression remained almost unchanged (Figure 1D).

Depleting circEEF2 inhibits PCa cell malignancy

si-circEEF2 targeting circEEF2 was synthesized and transfected into PC3 cells to specifically knock down circEEF2 expression (Figure 2A). Cell proliferation was examined using the CCK-8 assay alongside colony formation assay, revealing that the reduction of circEEF2 significantly diminished the proliferation capacity of PC3 cells (Figure 2 B, C). The findings from transwell assay revealed that reducing circEEF2 levels could prevent the migration and invasion of PC3 cells (Figure 2D). Our investigation focused on the impact of reducing circEEF2 levels on proteins related to epithelial mesenchymal transition markers (EMT) using protein blotting analysis, and the experimental results presented that knocking down circEEF2 upregulated E-cadherin and decreased vimentin (Figure 2E). Flow cytometry further indicated that knocking down circEEF2 significantly increased the apoptosis rate (Figure 2F).

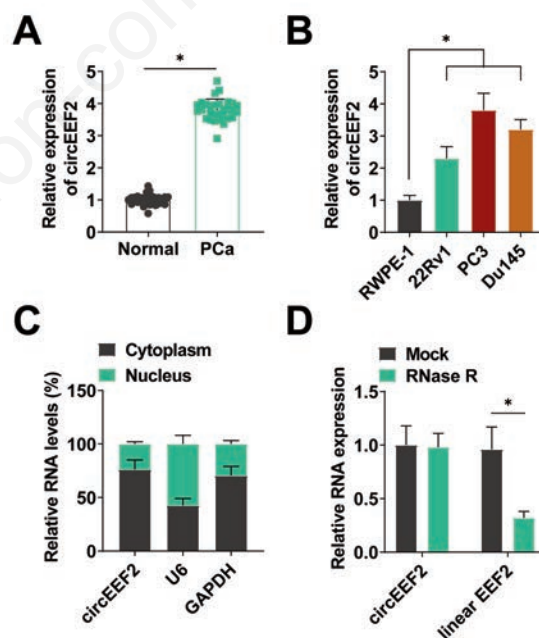


Figure 1. circEEF2 is highly expressed in PCa. **A,B)** RT-qPCR to detect circEEF2 in PCa tissues and PCa cell lines. **C)** Nucleoplasmic separation assay to detect circEEF2 in the cytoplasm and nucleus. **D)** RNase R treatment of total RNA in PC3 cells was followed by RT-qPCR to detect the levels of circEEF2 and linear EEF2. All experiments were repeated 3 times and data are shown as mean \pm SD. * $p < 0.05$.

CircEEF2 adsorbs miR-625-5p in PCa cells

We predicted possible miRNA targets of circEEF2 using bioinformatics tools. According to Circular RNA Interactome, miR-625-5p might be circEEF2's target (Figure 3A). miR-625-5p expression was detected by RT-qPCR in PCa tissues and cell lines (22Rv1, PC3, Du145). As measured, miR-625-5p was downregulated in PCa (Figure 3 B,C). Dual luciferase reporter gene experiments revealed a reduction in luciferase activity when miR-625-5p mimic and WT-circEEF2 were co-transfected, while co-transfection with MUT-circEEF2 had no effect (Figure 3D). Furthermore, miR-625-5p and circEEF2 interact in PCa cells as demonstrated by RNA-pull-down assays. The biotin-miR-625-5p-WT group enriched circEEF2 more than the biotin-miR-625-5p-MUT group (Figure 3E). FISH experiments demonstrated that circEEF2 was co-localized with miR-625-5p in the cytoplasm (Figure 3F). In addition, after knockdown of circEEF2, RT-qPCR found that circEEF2 depletion was able to upregulate miR-625-5p (Figure 3G).

Depleting miR-625-5p disrupts the action of circEEF2 depletion on cancer development

Investigating if circEEF2 promotes cancer in PC3 cells by absorbing miR-625-5p, we introduced si-circEEF2, either solely or in combination with a miR-625-5p inhibitor, into PC3 cells. RT-qPCR findings indicated that introducing si-circEEF2 elevated miR-625-5p levels, whereas the miR-625-5p inhibitor did not alter miR-625-5p expression (Figure 4A). circEEF2 depletion impeded cell proliferation, but miR-625-5p downregulation eliminated this effect (Figure 4 B,C). Meanwhile, when circEEF2 was knocked down, PC3 cells' migratory and invasive abilities were blocked, but they were restored when miR-625-5p was knocked down as well (Figure 4D). Further, miR-625-5p knockdown abolished the effect of circEEF2 depletion on EMT (Figure 4E) and apoptosis (Figure 4F).

TRPM2 is a direct target of miR-625-5p

According to the TargetScan database (<https://www.tar->

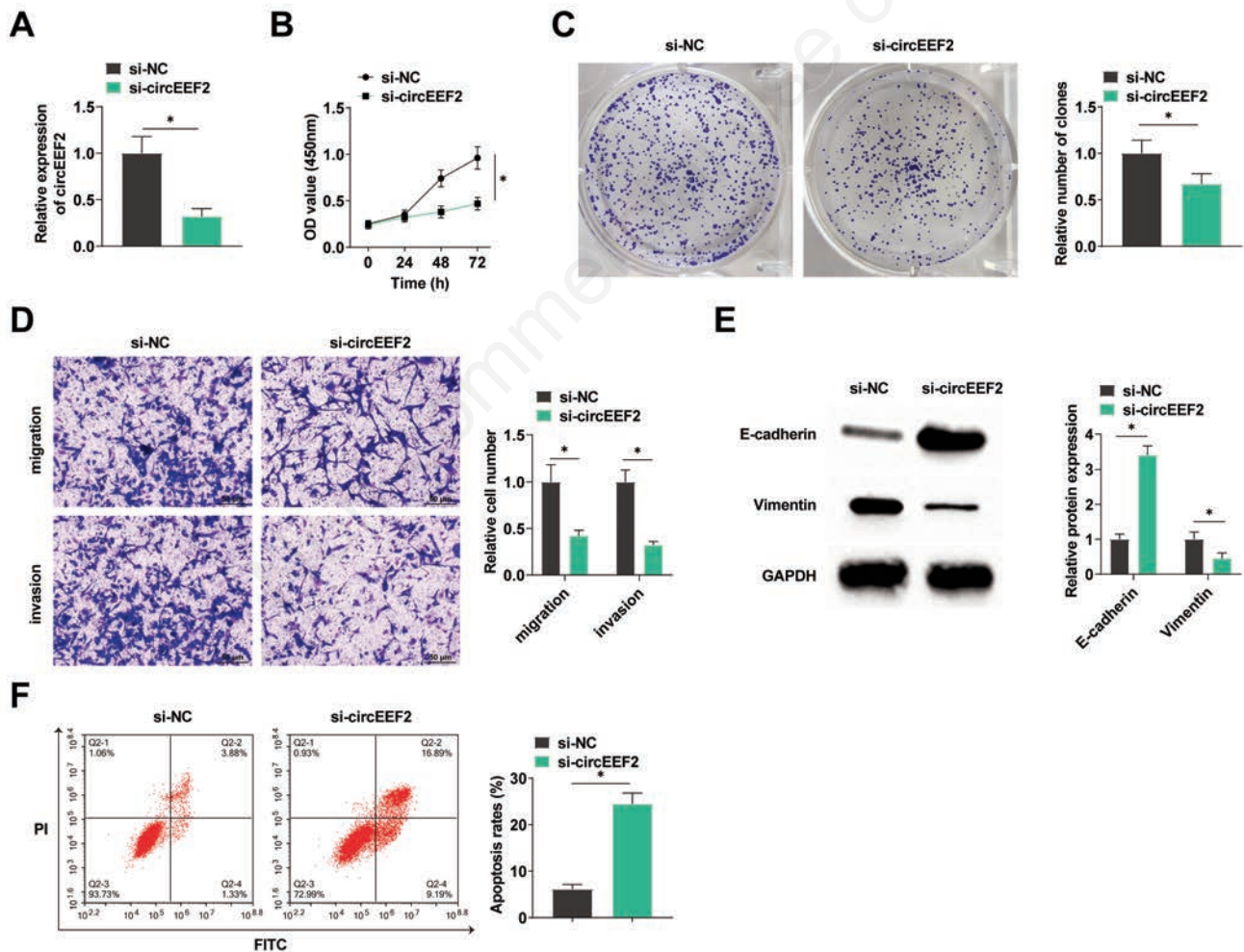


Figure 2. Knockdown of circEEF2 inhibits proliferation, migration, and invasion and promotes apoptosis of PCa cells. **A**) RT-qPCR to detect circEEF2 in PC3 cells. **B**) CCK-8 assay to detect PC3 cell proliferation. **C**) Colony formation assay to detect PC3 cell clone formation. **D**) Transwell assay to detect migratory and invasive ability of PC3 cells. **E**) Protein blotting to detect the E-cadherin and vimentin expression level. **F**) Flow cytometry to detect apoptosis of PC3 cells. All experiments were repeated 3 times and the data are shown as mean \pm SD. * $p < 0.05$.

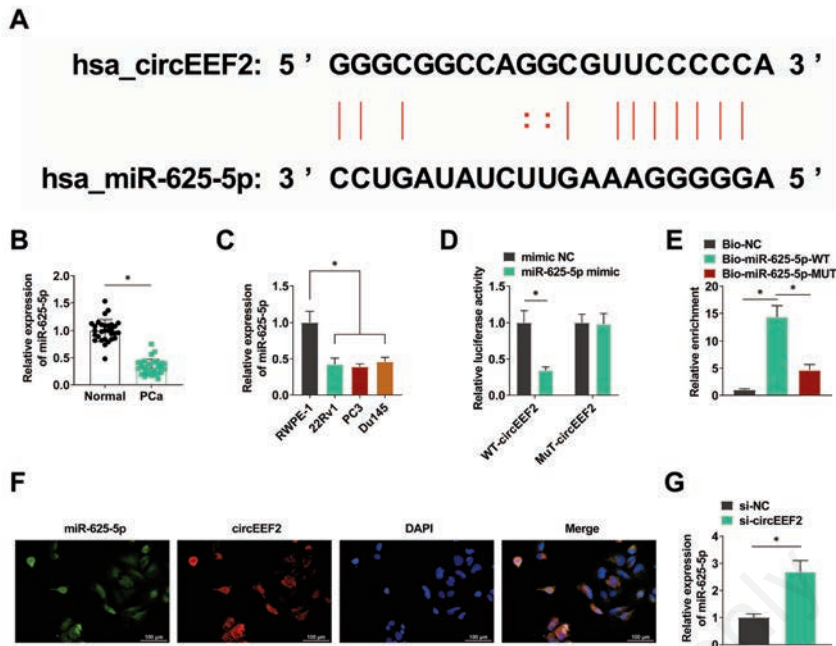


Figure 3. miR-625-5p is adsorbed by circEEF2. **A)** CircInteractome predicts the binding site of miR-625-5p to circEEF2. **B,C)** RT-qPCR to detect miR-625-5p expression in PCa tissues and cell lines. **D,E)** Dual-luciferase reporter gene assay and RNA-pull-down to validate the binding of circEEF2 to miR-625-5p. **F)** FISH to detect the co-localization of circEEF2 with miR-625-5p. **G)** RT-qPCR to detect miR-625-5p in PC3 cells. All experiments were repeated 3 times and data are shown as mean ± SD. **p*<0.05.

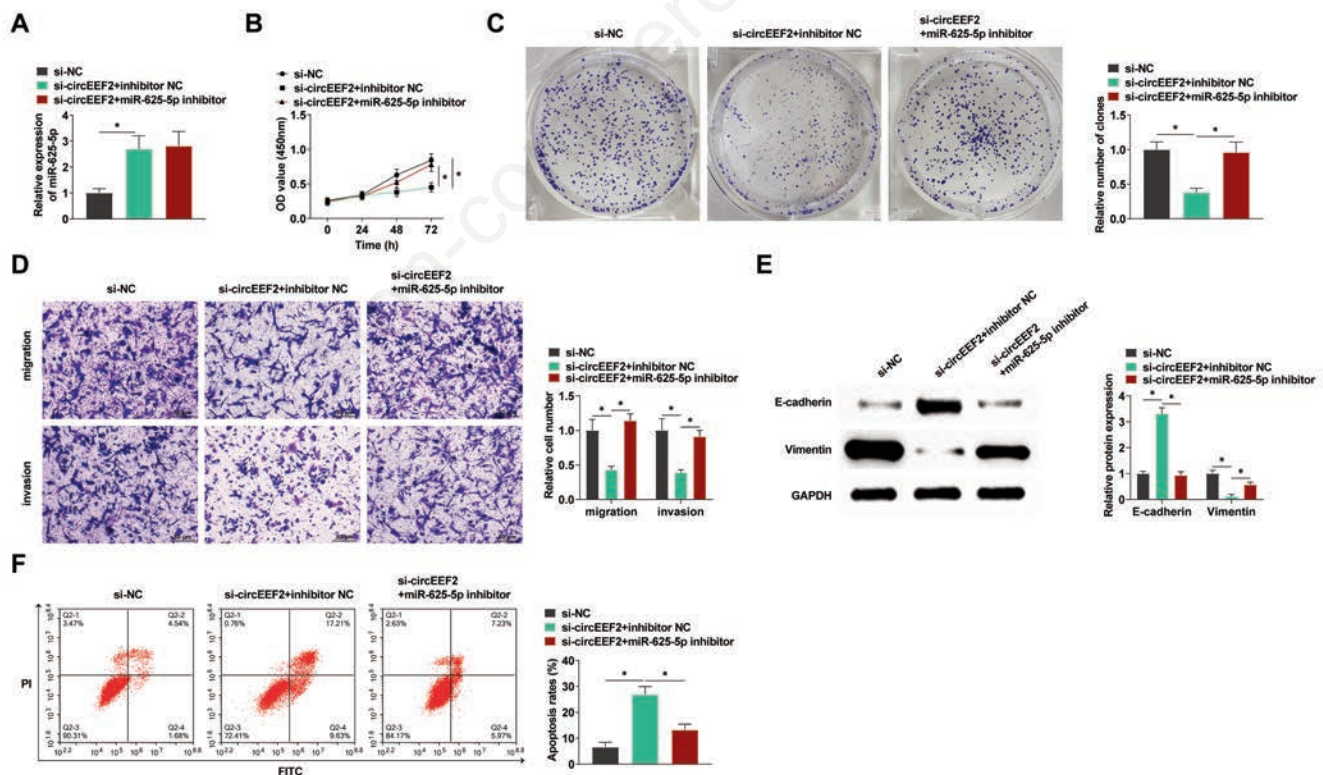


Figure 4. Knockdown of miR-625-5p reverses the inhibition of cancer development by knockdown of circEEF2. **A)** RT-qPCR to detect miR-625-5p in PC3 cells after transfection. **B,C)** CCK-8 assay with colony formation assay to detect proliferation of PC3 cells. **D)** Transwell assay to detect the migratory and invasive ability of PC3 cells. **E)** protein blotting to detect E-cadherin and vimentin expression level. **F)** Flow cytometry to detect apoptosis of PC3 cells. All experiments were repeated 3 times and the data are shown as mean ± SD. **p*<0.05.

getscan.org/), miR-625-5p was shown to have a possible binding relationship with TRPM2 mRNA, and the binding sites of both were predicted (Figure 5A). Elevated TRPM2 levels were measured in PCa tumor tissues (Figure 5B, C) and PCa cell lines (Figure 5 D,E). When miR-625-5p mimics and WT-TRPM2 were co-transfected, luciferase activity was reduced, whereas MUT-TRPM2 had no impact (Figure 5F). The biotin-miR-625-5p-WT group enriched more TRPM2 than the biotin-miR-625-5p-MUT group by the RNA-pull-down assay, which again confirmed that miR-625-5p and TRPM2 were able to bind in a targeted manner (Figure 5G). After transfection of PCa cells using miR-625-5p mimic and inhibitor, respectively, RT-qPCR and protein blotting results quantified that miR-625-5p mimic lowered TRPM2 levels, whereas miR-625-5p inhibitor further upregulated TRPM2 (Figure 5 H,I).

TRPM2 upregulation impairs the ability of circEEF2 depletion to inhibit cancer development

We transfected si-circEEF2 alone or together with TRPM2 overexpressing plasmid into PC3 cells and functional rescue experiments were performed. RT-qPCR and Western blotting results showed that si-circEEF2 decreased TRPM2 expression, while co-transfection of pc-TRPM2 increased TRPM2 expression (Figure 6 A,B). Increasing TRPM2 impaired the impact of knock-down of circEEF2 on PC3 cell proliferation (Figure 6 C,D), migra-

tion and invasion (Figure 6E), E-cadherin and vimentin levels (Figure 6F), and apoptosis (Figure 6G).

circEEF2 regulates miR-625-5p/TRPM2 to activate the Hh pathway and promote mitochondrial stress

GLI1 and GLI2, key factors of the Hh signaling pathway, were observed in PC3 cells before and after transfection. protein blotting results showed that GLI1 and GLI2 expression were downregulated by knocking down circEEF2, however, inhibition of miR-625-5p or overexpression of TRPM2 was able to rescue the downregulation of GLI1 and GLI2 (Figure 7A). Mitochondrial stress leads to drug resistance in cancer cells, which promotes cancer development. For mitochondrial stress, the role of circEEF2/miR-625-5p/TRPM2 axis was explored under the same transfection conditions described above. Alterations in mitochondrial membrane potential (MMP) were gauged using the fluorescent JC-1 dye. When MMP is low, JC-1 dye mainly exists in a monomeric form with green fluorescence, but at elevated MMP levels, it transitions to red fluorescence, causing JC-1 to cluster. Our results show that circEEF2 depletion upregulated MMP, yet inhibition of miR-625-5p or overexpression of TRPM2 downregulated MMP again (Figure 7B). Mitochondria are important sites for ROS production; therefore we also assessed the effect on mitochondrial stress by evaluating intracellular ROS levels by fluorescence microscopy,

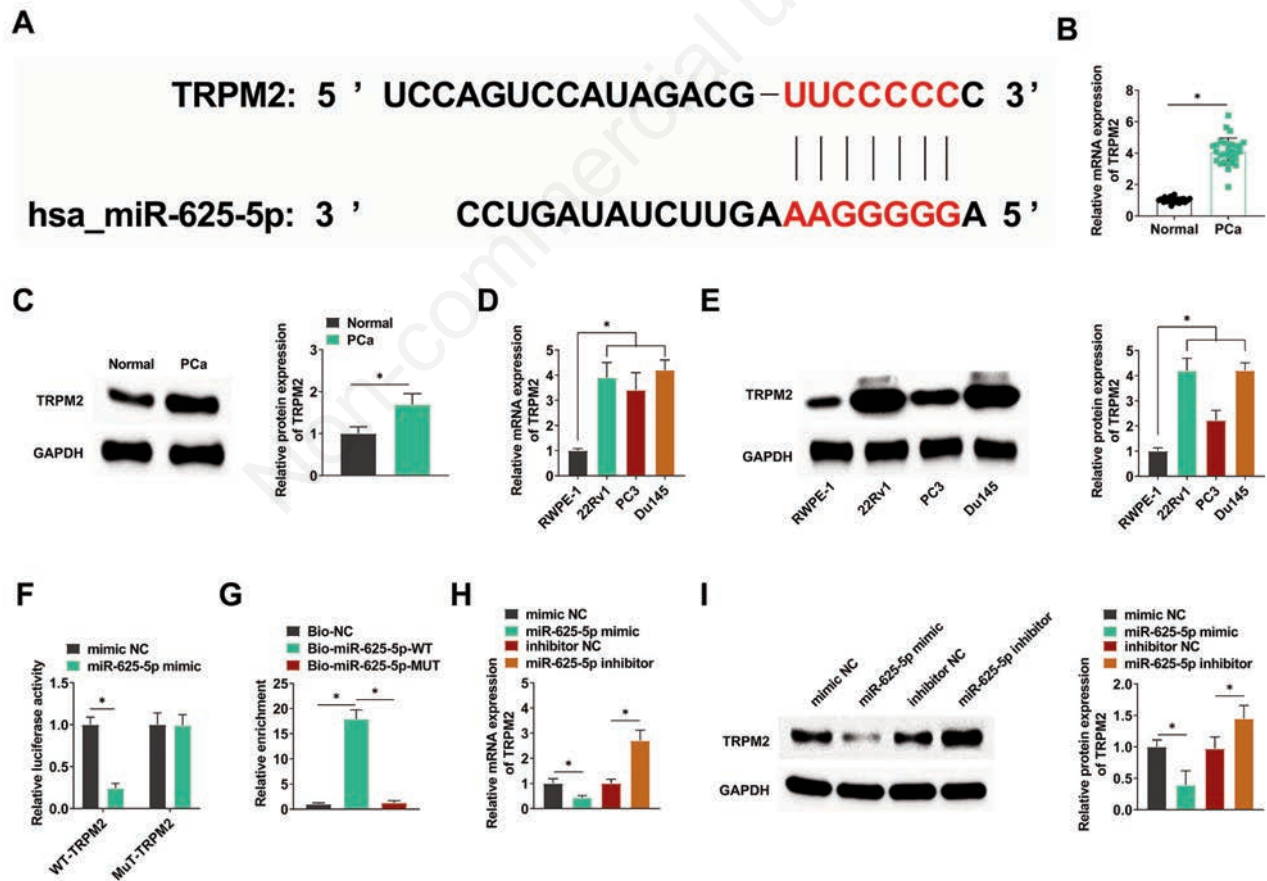


Figure 5. TRPM2 is a direct target of miR-625-5p. **A)** Prediction of the binding site between miR-625-5p and TRPM2. **B,C)** RT-qPCR and protein blotting to detect TRPM2 in PCa tumor tissues. **D,E)** RT-qPCR and protein blotting to detect TRPM2 in PCa cell lines. **F,G)** Dual-luciferase reporter gene analysis and RNA-pull-down assay to verify the target binding between miR-625-5p and TRPM2. **H,I)** RT-qPCR and protein blotting to detect TRPM2 in PC3 cells after addition of miR-625-5p mimic and inhibitor, respectively. All experiments were repeated 3 times and data are shown as mean \pm SD. * $p < 0.05$.

which showed that intracellular ROS expression was decreased by knockdown of circEEF2, and then increased again by co-transfection of miR-625-5p inhibitor or TRPM2 overexpression plasmid (Figure 7C). Mitochondrial stress-related proteins NDUFB8 and COX4 were continued to be detected by protein blotting (Figure 7D), and γ -H2AX in PC3 cells was detected by immunofluorescence (Figure 7E). The results showed the same trend as above, and the downregulation of NDUFB8, COX4 and γ -H2AX in PC3 cells by knockdown of circEEF2 was counteracted by co-transfection of miR-625-5p inhibitor or TRPM2 overexpression plasmid.

Loss of circEEF2 inhibits PCa growth *in vivo*

A subcutaneous injection of PC3 cells transfected with si-circEEF2 or si-NC was performed on BALB/c nude mice. Images of the xenografted tumors are shown in Figure 8A. Tumors knocked down by circEEF2 were significantly reduced in volume and weight as the number of days increased (Figure 8 B,C). protein blotting results demonstrated that TRPM2, GLI1 and GLI2 proteins were also significantly reduced in the tumor tissues of mice knocked down by circEEF2 (Figure 8D), which *in vivo* re-validat-

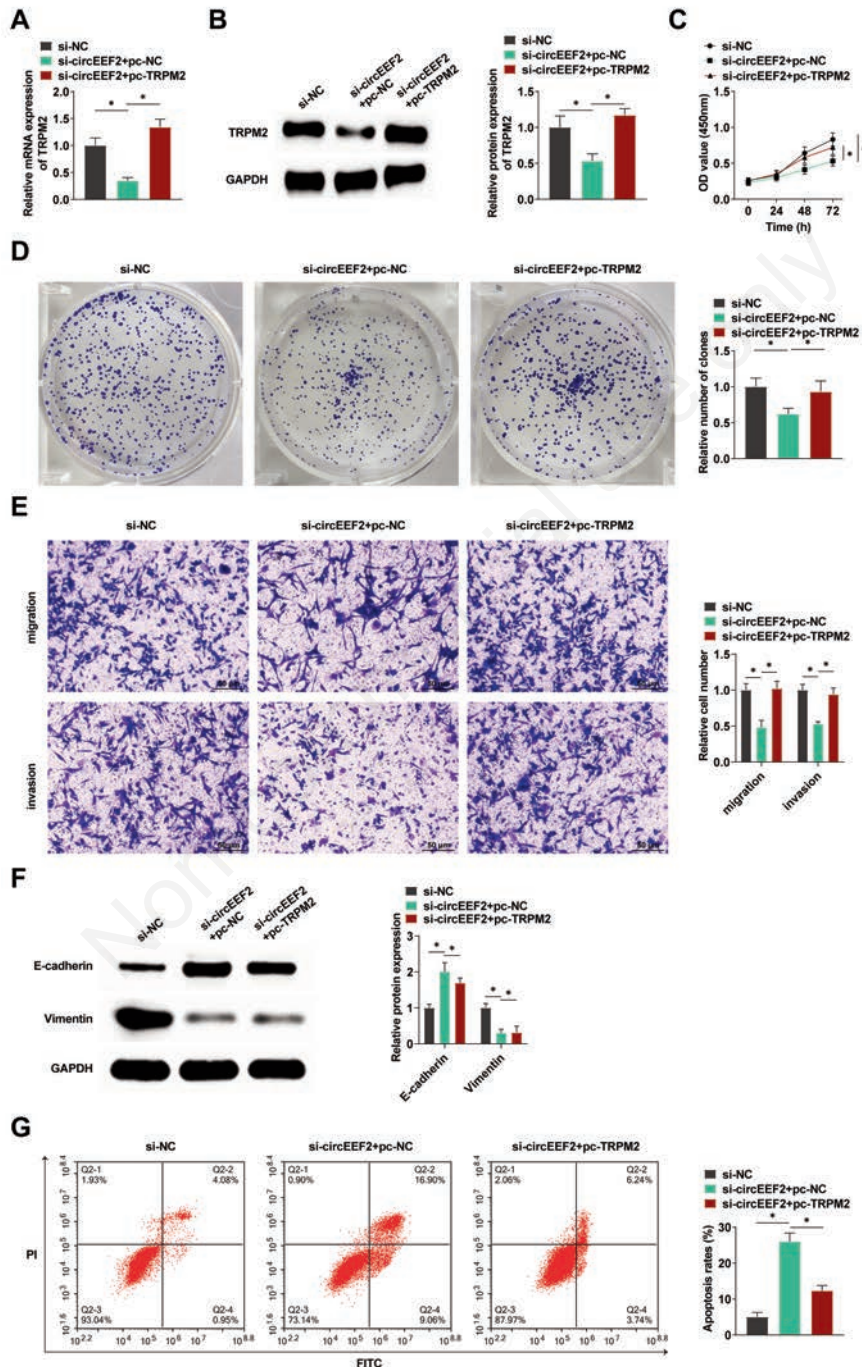


Figure 6. Overexpression of TRPM2 reverses knockdown of circEEF2 to inhibit cancer development. **A,B**) RT-qPCR and protein blotting to detect TRPM2 in PC3 cells after transfection. **C,D**) CCK-8 assay and colony formation assay to detect proliferation of PC3 cells. **E**) Transwell to detect the migratory and invasive ability of PC3 cells. **F**) Protein blotting to detect E-cadherin and vimentin in PC3 cells. **G**) Flow cytometry to detect apoptosis of PC3 cells. All experiments were repeated 3 times and the data are shown as mean \pm SD. * p <0.05.

ed the ability of circEEF2 to affect the TRPM2 activation of the Hh signaling pathway.

Discussion

Existing studies have shown that circRNAs are specifically expressed in many diseases and play important regulatory roles in disease development, among which the study of circRNAs in tumors has been reported most frequently. Many experiments have demonstrated that circRNAs play an important role in tumors, such as liver cancer,²⁹ gastric cancer,³⁰ lung cancer,³¹ breast cancer,³² cervical cancer,³³ and so on. circRNAs are believed to play a key role in the progression of PCA.³⁴⁻³⁶ Similarly, the results of this study confirmed the presence and elevated expression of a novel circRNA (circEEF2) in PCA. Both loss-of-function and gain-of-function studies identified an oncogenic role for circEEF2 in PCA.

There is a close correlation between circRNA function and its subcellular localization.³⁷ Studies have shown that circRNAs located

in the cytoplasm play a role mainly by binding to miRNAs, while RNAs located in the nucleus are mainly involved in the regulation of transcription or the regulation of gene splicing.³⁸ Most of the circRNAs in the cytoplasm have a base sequence that binds to miRNA, which can act as a competitive endogenous RNA to compete for binding miRNA, relieve the inhibition of miRNA on target genes, and then affect the process of disease development.³⁹ As circEEF2 is mostly localized in the cytoplasm of PC3 cells, it may serve as an endogenous miRNA sponge. Functionally, circEEF2 depletion impeded the proliferation, migration and invasion of PCA cells and promoted apoptosis. Then, circEEF2 may be a target of miR-625-5p. MiR-625-5p has been shown to inhibit the proliferation and metastasis of tumor cells in many cancers.^{23,40,41} Our study found that miR-625-5p was lowly expressed in PCA and miR-625-5p inhibitor was able to reverse the therapeutic effect of circEEF2 depletion on PCA. The above results confirm that circEEF2 plays a role as a ceRNA in PCA and that it promotes PCA genesis through interaction with miR-625-5p.

A calcium-permeable ion channel, TRPM2, is a potential prognostic marker for PCA.^{42,43} The TRPM2 gene is highly expressed in

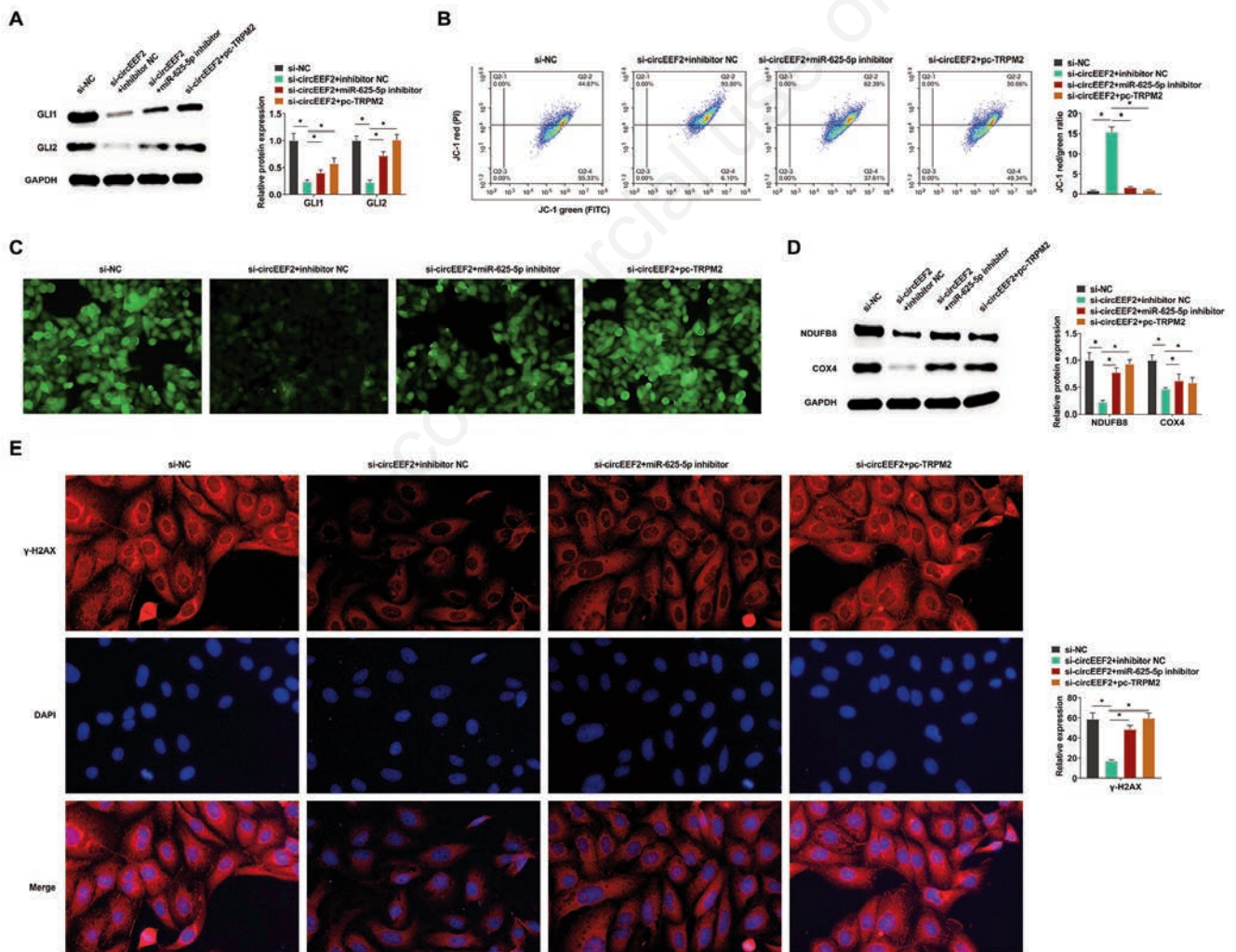


Figure 7. circEEF2 regulates miR-625-5p/TRPM2 to activate the Hh signaling pathway and promote mitochondrial stress. **A)** Protein blotting to explore the relationship between miR-625-5p, TRPM2 and Hh pathway proteins GLI1 and GLI2. **B)** JC-1 to determine MMP changes in PC3 cells. **C)** Fluorescent probe to detect ROS in PC3 cells. **D)** protein blotting to detect NDUFB8 and COX4. **E)** Immunofluorescence detection of γ -H2AX expression in PC3 cells. All experiments were repeated 3 times and data are shown as mean \pm SD. * p <0.05.

a variety of tumor types, including PCa.⁴⁴⁻⁴⁶ In this study, TRPM2 is a target of miR-625-5p. It was also found that miR-625-5p mimics inhibited TRPM2 expression, whereas miR-625-5p inhibitor promoted its expression. The study of Shi *et al.* reported that TRPM2 can promote the proliferation of PCa cells.⁴⁷ In our study, we also found that overexpression of TRPM2 can inhibit the progression of cancer. Overexpression of TRPM2 reversed the therapeutic effect of knockdown of circEEF2 on PCa.

The Hh pathway and mitochondrial stress have been poorly studied in PCa, yet they are important regulators in cancer. As cancer progresses, Hh signaling is aberrantly activated and participates in cell proliferation, invasion, and metastasis, blocking cell death signaling, and deregulating metabolism.⁴⁸ Furthermore, cancer cells suffer from mitochondrial stress due to unchecked cell growth and ROS production, resulting in the destruction of mitochondrial DNA and crucial mitochondrial proteins, culminating in mitochondrial malfunction.⁴⁹ The proliferative capacity of cancer cells relies on amino acids, nucleotides, and cholesterol produced by functioning mitochondria. circIPO11 is able to drive the self-renewal of hepatocellular carcinoma initiating cells through the Hh signaling.⁵⁰ Similarly, in our study, circEEF2 also regulated the Hh pathway. Differently, that study found that circIPO11 initiated self-renewal of cancer stem cells by activating the Hh signaling. In contrast, our study found that circEEF2/miR-625-5p/TRPM2 promoted cancer development in PCa by activating the Hh pathway and causing mitochondrial stress and dysfunction. We investigated the effects of circEEF2/miR-625-5p/TRPM2 on the Hh pathway GLI1 and GLI2 proteins, and the functional mitochondrial proteins NDUFB8 and COX4, as well as on the intracellular production of ROS, changes in the mitochondrial membrane potential, and mitochondrial damage marker γ -H2AX.

In short, circEEF2 is upregulated and exerts an oncogenic role in PCa. Mechanistically, circEEF2 sponges miR-625-5p to promote TRPM2 expression, which activates the Hh pathway and

mitochondrial stress. However, there are still limitations in this study. First of all, although this study carried out subcutaneous tumor formation experiments in nude mice, no *in vivo* animal metastasis model experiments were carried out. In addition, the study found the role of circEEF2 in PCa, but did not further analyze the clinical correlation. However, for the first time, we found the mechanism of circEEF2/miR-625-5p/TRPM2 axis in the development of PCa. These findings suggest that circTENM3 may be a promising PCa biomarker, and circEEF2 may be a potential therapeutic target for PCa patients.

References

- Feng H, Deng Z, Peng W, Wei X, Liu J, Wang T. Circular RNA EPHA3 suppresses progression and metastasis in prostate cancer through the miR-513a-3p/BMP2 axis. *J Transl Med* 2023;21:288.
- Siegel RL, Miller KD, Fuchs HE, Jemal A. Cancer statistics, 2022. *CA Cancer J Clin* 2022;72:7-33.
- Nuhn P, De Bono JS, Fizazi K, Freedland SJ, Grilli M, Kantoff PW, et al. Update on systemic prostate cancer therapies: management of metastatic castration-resistant prostate cancer in the era of precision oncology. *Eur Urol* 2019;75:88-99.
- He H, Li J, Luo M, Wei Q. Inhibitory role of circRNA_100395 in the proliferation and metastasis of prostate cancer cells. *J Int Med Res* 2021;49:300060521992215.
- Hussain M, Fizazi K, Saad F, Rathenborg P, Shore N, Ferreira U, et al. Enzalutamide in men with nonmetastatic, castration-resistant prostate cancer. *N Engl J Med* 2018;378:2465-74.
- Rajappa A, Banerjee S, Sharma V, Khandelia P. Circular RNAs: emerging role in cancer diagnostics and therapeutics. *Front Mol Biosci* 2020;7:577938.
- Chen LL. The biogenesis and emerging roles of circular RNAs.

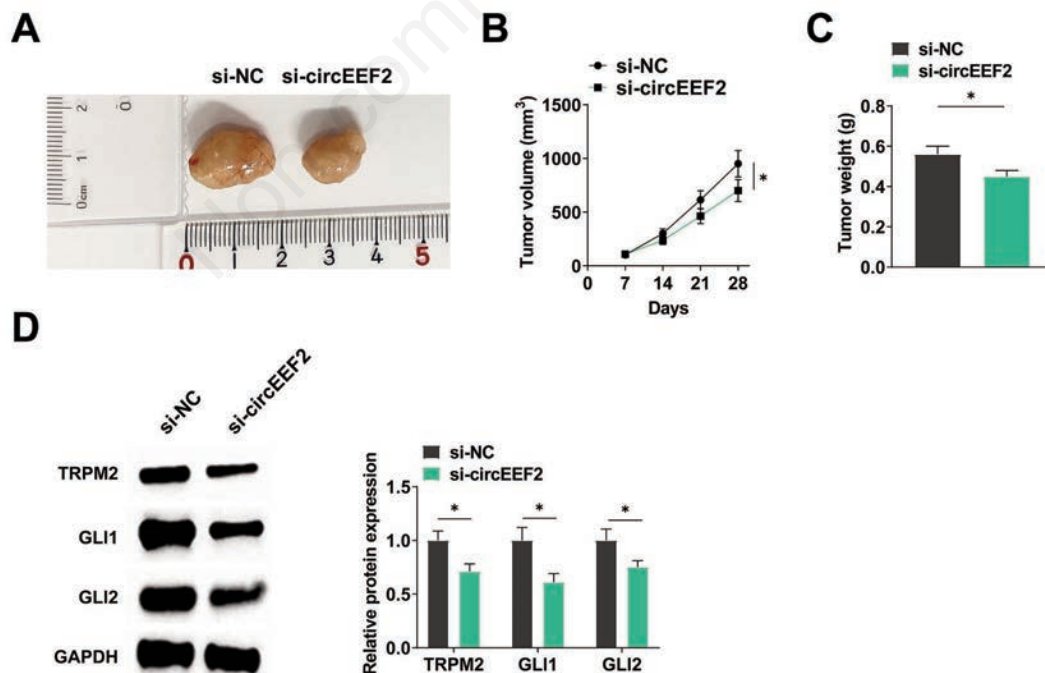


Figure 8. Knockdown of circEEF2 inhibits PCa growth *in vivo*. **A)** Images of xenograft tumors. **B)** Tumor volume detected weekly. **C)** Tumor weight (day 28). **D)** TRPM2, GLI1 and GLI2 proteins in xenograft tumor tissues detected by protein blotting. All experiments were repeated 3 times and data are shown as mean \pm SD. * $p < 0.05$.

- Nat Rev Mol Cell Biol 2016;17:205-11.
8. Salzman J. Circular RNA expression: its potential regulation and function. *Trends Genet* 2016;32:309-16.
 9. Chen S, Huang V, Xu X, Livingstone J, Soares F, Jeon J, et al. Widespread and functional rna circularization in localized prostate cancer. *Cell* 2019;176:831-43.e22.
 10. Hua JT, Chen S, He HH. Landscape of noncoding RNA in prostate cancer. *Trends Genet* 2019;35:840-51.
 11. Vo JN, Cieslik M, Zhang Y, Shukla S, Xiao L, Zhang Y, et al. The landscape of circular RNA in cancer. *Cell* 2019;176:869-81.e13.
 12. Li P, Wang Z, Li S, Wang L. Circ_0006404 accelerates prostate cancer progression through regulating miR-1299/CFL2 signaling. *Onco Targets Ther* 2021;14:83-95.
 13. Shen Z, Zhou L, Zhang C, Xu J. Reduction of circular RNA Foxo3 promotes prostate cancer progression and chemoresistance to docetaxel. *Cancer Lett* 2020;468:88-101.
 14. Xu S, Lian Z, Zhang S, Xu Y, Zhang H. CircGNG4 promotes the progression of prostate cancer by sponging miR-223 to enhance EYA3/c-myc expression. *Front Cell Dev Biol* 2021;9:684125.
 15. Rupaimoole R, Slack FJ. MicroRNA therapeutics: towards a new era for the management of cancer and other diseases. *Nat Rev Drug Discov* 2017;16:203-22.
 16. Yong M, Hu J, Zhu H, Jiang X, Gan X, Hu L. Circ-EEF2 facilitated autophagy via interaction with mir-6881-3p and ANXA2 in EOC. *Am J Cancer Res* 2020;10:3737-51.
 17. Rishabh K, Khadilkar S, Kumar A, Kalra I, Kumar AP, Kunnumakkara AB. MicroRNAs as modulators of oral tumorigenesis-A focused review. *Int J Mol Sci* 2021;22:2561.
 18. Maleki M, Golchin A, Javadi S, et al. Role of exosomal miRNA in chemotherapy resistance of Colorectal cancer: A systematic review. *Chem Biol Drug Dev* 2023;101:1096-112.
 19. Mok ETY, Chitty JL, Cox TR. miRNAs in pancreatic cancer progression and metastasis. *Clin Exp Metastasis* 2024;41:163-86.
 20. Aktan Ç, Çal Ç, Kaymaz B, Selvi Günel N, Kıpçak S, Özel B, et al. Functional roles of miR-625-5p and miR-874-3p in the progression of castration resistant prostate cancer. *Life Sci* 2022;301:120603.
 21. Shang T, Zhou X, Chen W. LINC01123 promotes the progression of colorectal cancer via miR-625-5p/LASP1 axis. *Cancer Biother Radiopharm* 2021;36:765-73.
 22. Chen Z, Wu H, Zhang Z, Li G, Liu B. LINC00511 accelerated the process of gastric cancer by targeting miR-625-5p/NFIX axis. *Cancer Cell Int* 2019;19:351.
 23. Li H, Zheng S, Wan T, Yang X, Ouyang Y, Xia H, Wang X. Circular RNA circ_0000212 accelerates cervical cancer progression by acting as a miR-625-5p sponge to upregulate PTP4A1. *Anticancer Drugs* 2023;34:659-68.
 24. Tektemur A, Ozaydin S, Etem Onalan E, Kaya N, Kuloglu T, Hanifi Ozercan I, et al. TRPM2 mediates disruption of autophagy machinery and correlates with the grade level in prostate cancer. *J Cancer Res Clin Oncol* 2019;145:1297-311.
 25. Gonnissen A, Isebaert S, Haustermans K. Hedgehog signaling in prostate cancer and its therapeutic implication. *Int J Mol Sci* 2013;14:13979-4007.
 26. Karhadkar SS, Bova GS, Abdallah N, Dhara S, Gardner D, Maitra A, et al. Hedgehog signalling in prostate regeneration, neoplasia and metastasis. *Nature* 2004;431:707-12.
 27. O'Malley J, Kumar R, Inigo J, Yadava N, Chandra D. Mitochondrial stress response and cancer. *Trends Cancer* 2020;6:688-701.
 28. Civenni G, Bosotti R, Timpanaro A, Vázquez R, Merulla J, Pandit S, et al. Epigenetic control of mitochondrial fission enables self-renewal of stem-like tumor cells in human prostate cancer. *Cell Metab* 2019;30:303-18.e6.
 29. Zhang Y, Li J, Cui Q, Hu P, Hu S, Qian Y. Circular RNA hsa_circ_0006091 as a novel biomarker for hepatocellular carcinoma. *Bioengineered* 2022;13:1988-2003.
 30. Li M, Liu M, Bin Y, Xia J. Prediction of circRNA-disease associations based on inductive matrix completion. *BMC Med Genomics* 2020;13:42.
 31. Zheng H, Cao Z, Lv Y, Cai X. WTAP-mediated N6-methyladenine modification of circEEF2 promotes lung adenocarcinoma tumorigenesis by stabilizing CANT1 in an IGF2BP2-dependent manner. *Mol Biotechnol* 2024. Online ahead of print.
 32. Yang R, Chen H, Xing L, Wang B, Hu M, Ou X, et al. Hypoxia-induced circWSB1 promotes breast cancer progression through destabilizing p53 by interacting with USP10. *Mol Cancer* 2022;21:88.
 33. Najafi S. Circular RNAs as emerging players in cervical cancer tumorigenesis; A review to roles and biomarker potentials. *Int J Biol Macromol* 2022;206:939-53.
 34. Zhang P, Gao H, Yan R, Yu L, Xia C, Yang D. has_circ_0070512 promotes prostate cancer progression by regulating the miR-338-3p/hedgehog signaling pathway. *Cancer Sci* 2023;114:1491-506.
 35. Qi JC, Yang Z, Lin T, Ma L, Wang YX, Zhang Y, et al. CDK13 upregulation-induced formation of the positive feedback loop among circCDK13, miR-212-5p/miR-449a and E2F5 contributes to prostate carcinogenesis. *J Exp Clin Cancer Res* 2021;40:2.
 36. Shi J, Liu C, Chen C, Guo K, Tang Z, Luo Y, et al. Circular RNA circMBOAT2 promotes prostate cancer progression via a miR-1271-5p/mTOR axis. *Aging (Albany NY)* 2020;12:13255-80.
 37. Esteller M. Non-coding RNAs in human disease. *Nat Rev Genet* 2011;12:861-74.
 38. Li J, Sun D, Pu W, Wang J, Peng Y. Circular RNAs in cancer: biogenesis, function, and clinical significance. *Trends Cancer* 2020;6:319-36.
 39. Anastasiadou E, Faggioni A, Trivedi P, Slack FJ. The nefarious nexus of noncoding RNAs in cancer. *Int J Mol Sci* 2018;19:2072.
 40. Samieyan Dehkordi S, Mousavi SH, Ebrahimi M, Alizadeh SH, Hedayati Asl AA, Mohammad M, et al. Upregulation of hsa-miR-625-5p inhibits invasion of acute myeloid leukemia cancer cells through ILK/AKT pathway. *Cell J* 2022;24:76-84.
 41. Qi L, Sun B, Yang B, Lu S. CircMMP11 regulates proliferation, migration, invasion, and apoptosis of breast cancer cells through miR-625-5p/ZEB2 axis. *Cancer Cell Int* 2021;21:133.
 42. Tektemur A, Ozaydin S, Etem Onalan E, Kaya N, Kuloglu T, Ozercan İ H, et al. TRPM2 mediates disruption of autophagy machinery and correlates with the grade level in prostate cancer. *J Cancer Res Clin Oncol* 2019;145:1297-311.
 43. Cheung JY, Miller BA. Transient receptor potential-melastatin channel family member 2: friend or foe. *Trans Am Clin Climatol Assoc* 2017;128:308-29.
 44. Orfanelli U, Jachetti E, Chiacchiera F, Grioni M, Brambilla P, Briganti A, et al. Antisense transcription at the TRPM2 locus as a novel prognostic marker and therapeutic target in prostate cancer. *Oncogene* 2015;34:2094-102.
 45. Almasi S, Kennedy BE, El-Aghil M, Sterea AM, Gujar S, Partida-Sánchez S, et al. TRPM2 channel-mediated regulation of autophagy maintains mitochondrial function and promotes gastric cancer cell survival via the JNK-signaling pathway. *J Biol Chem* 2018;293:3637-50.
 46. Almasi S, Long CY, Sterea A, Clements DR, Gujar S, El Hiani Y. TRPM2 silencing causes G2/M arrest and apoptosis in lung

- cancer cells via increasing intracellular ROS and RNS levels and activating the JNK pathway. *Cell Physiol Biochem* 2019;52:742-57.
47. Zeng X, Sikka SC, Huang L, Sun C, Xu C, Jia D, et al. Novel role for the transient receptor potential channel TRPM2 in prostate cancer cell proliferation. *Prostate Cancer Prostatic Dis* 2010;13:195-201.
48. Hanna A, Shevde LA. Hedgehog signaling: modulation of cancer properties and tumor microenvironment. *Mol Cancer* 2016;15:24.
49. Shemorry A, Harnoss JM, Guttman O, Marsters SA, Kómúves LG, Lawrence DA, et al. Caspase-mediated cleavage of IRE1 controls apoptotic cell commitment during endoplasmic reticulum stress. *Elife* 2019;8:e47084.
50. Gu Y, Wang Y, He L, Zhang J, Zhu X, Liu N, et al. Circular RNA circIPO11 drives self-renewal of liver cancer initiating cells via Hedgehog signaling. *Mol Cancer* 2021;20:132.

Non-commercial use only

Received: 20 May 2024. Accepted: 30 August 2024.

This work is licensed under a Creative Commons Attribution-NonCommercial 4.0 International License (CC BY-NC 4.0).

©Copyright: the Author(s), 2024

Licensee PAGEPress, Italy

European Journal of Histochemistry 2024; 68:4063

doi:10.4081/ejh.2024.4063

Publisher's note: all claims expressed in this article are solely those of the authors and do not necessarily represent those of their affiliated organizations, or those of the publisher, the editors and the reviewers. Any product that may be evaluated in this article or claim that may be made by its manufacturer is not guaranteed or endorsed by the publisher.